Nonlinear Dyn (2017) 90:971–981
DOI 10.1007/s11071-017-3705-9

ORIGINAL PAPER

Mathematical modelling and control of a nonholonomic spherical robot on a variable-slope inclined plane using terminal sliding mode control

M. Roozegar · M. Ayati · M. J. Mahjoob

Received: 18 November 2016 / Accepted: 27 July 2017 / Published online: 5 August 2017

Abstract Motion analysis and control of a pendulum-driven spherical robot (PDSR) on an inclined plane with a variable slope is investigated. Firstly, the mathematical model of a PDSR on a variable-slope inclined plane is deduced applying a Lagrangian formulation. Afterwards, in the presence of an unknown external disturbance, the terminal sliding mode control (TSMC) technique is employed to stabilize the robot on the inclined plane, while the plane is still moving. In other words, the terminal sliding mode disturbance observer is used to estimate the unknown disturbance. Based on the disturbance estimation, the TSMC scheme is established to control the single-input and single-output nonlinear system with control singularity and an unknown nonsymmetric control input saturation. In fact, a compound disturbance is defined and estimated, which includes the external disturbance, the control singularity and the unknown input saturation. Simulations are then conducted to validate the proposed approach for motion control of a PDSR on a variable-slope inclined plane with an unknown external disturbance and nonsymmetric input limits.

Keywords Terminal sliding mode control · Uncertain nonlinear systems · Unknown input saturation and disturbance estimation · Spherical robot · Inclined plane

M. Roozegar (✉)
Department of Mechanical Engineering, Centre for Intelligent Machines (CIM), McGill University, Montréal, Canada
e-mail: roozegar@cim.mcgill.ca

M. Ayati
School of Mechanical Engineering, University of Tehran, Tehran, Iran

M. J. Mahjoob
Centre for Mechatronics and Intelligent Machines, School of Mechanical Engineering, University of Tehran, Tehran, Iran

List of symbols

ϕ	Rotation of the spherical shell w.r.t. the (inclined) plane
β	Rotation of the main shaft w.r.t. the spherical shell
θ	Instantaneous angle of the pendulum w.r.t. the perpendicular to the (inclined) plane
α	Angle of the inclined plane
m_{p}	Mass of the pendulum
m_{s}	Mass of the spherical shell
M	Mass of the whole robot
I_{A}	Spherical shell moment of inertia about point A (centre)
I_{C}	Spherical shell moment of inertia about point C (contact point)
ρ	Radius of the spherical shell
r	Radius of the pendulum
r_G	Radius of the robot mass centre
$\boldsymbol{q}$	Vector of generalized coordinates, i.e., $\boldsymbol{q} = [\phi \quad \theta]^{\mathrm{T}}$

$\boldsymbol{Q}$	Vector of generalized forces, i.e., $\boldsymbol{Q} = \begin{bmatrix} Q_\phi & Q_\theta \end{bmatrix}^{\mathrm{T}}$
T	Total kinetic energy of the system
V	Total potential energy of the system
$\mathcal{L}$	Lagrangian, i.e., $\mathcal{L} = T - V$
T_{p}	Kinetic energy of the pendulum
T_{s}	Kinetic energy of the spherical shell
$\boldsymbol{\omega}_{\mathrm{s}}$	Angular velocity of the spherical shell
$\boldsymbol{V}_{\mathrm{A}}$	Velocity of point A (shell centre)
$\boldsymbol{V}_{\mathrm{C}}$	Velocity of point C (contact point)
$\boldsymbol{V}_{\mathrm{A/C}}$	Velocity of point A w.r.t. point C
$\boldsymbol{V}_{\mathrm{p}}$	Velocity of the pendulum
$\boldsymbol{V}_{\mathrm{p/A}}$	Velocity of the pendulum w.r.t. point A
x	Position of the robot on the inclined plane
x_0	Initial position of the robot on the inclined plane
g	Earth gravitational acceleration
$(\boldsymbol{i}, \boldsymbol{j}, \boldsymbol{k})$	Unit vectors in x, y and z directions
W	Work done by external forces/moments
τ_{m}	Torque of the motor
θ_{e}	Desired angle for θ in the equilibrium state of the robot
$\boldsymbol{x}$	Vector of state variables, i.e., $\boldsymbol{x} = [x_1 x_2 \ldots x_n]^{\mathrm{T}}$
u	Control input
$u_{\min}, u_{\max}$	Lower and upper limits of the control input
y	Output of the system
y_d	Desired output
d	Unknown external disturbance
D	Compound disturbance
$\widehat{D}$	Estimated compound disturbance
$\tau, k, \gamma, \epsilon, p_0, q_0, p_i, q_i, \alpha_i, \beta_i, \delta, \mu$	Controller and estimator design parameters
sign $(*)$	Sign function

1 Introduction

A pendulum-driven spherical robot (PDSR) moves by changing the position of its mass centre. Because of the spherical shape, these robots can be used in unfriendly or harsh environments, such as outer planets, deserts and earthquake ruins, for doing exploration or reconnaissance tasks [1–5]. Spherical robots are nonholonomic and nonlinear systems. Thus, the modelling and control of these robots are very challenging. Although extensive research has been conducted in this area, there are shortcomings in most of the existing studies; lack of knowledge warrants further work [6,7].

Li and Canny [8] established a three-step technique for motion planning of a sphere on a flat surface, including both position and orientation convergence. Mojabi [9] derived the dynamics model of a spherical robot, considering a chained system, and also, studied its algorithmic motion planning. Bhattacharya and Agrawal [10,11] built the first-order mathematical model of a kind of spherical robot applying the nonslip constraint and conservation of the angular momentum. The authors reported simulations and experimental results. Halme et al. [12,13] deduced the model of a spherical mobile robot and then dealt with the rolling ahead motion. However, the steering motion was not considered. Bicchi et al. [14,15] developed a quasi-static kinematic model and a planar Lagrangian dynamic model of a spherical robot. Nonetheless, research demonstrated that those models were only valid under limited circumstances. Joshi et al. [16,17] established the kinematics model of a spherical robot using Euler parameters and also proved its controllability. Using a Lagrangian formulation, Liu et al. [18] derived a simplified dynamics model of a spherical robot by input-state linearization. Based on the quasi-velocity, Qiang et al. [19] built the dynamics model of BHQ-1 spherical robot applying the Lagrange–d'Alembert formula, and then, based on a back-stepping method, the dynamic trajectory tracking problem of BHQ-2 was investigated [20]. Using the theory of nonholonomic systems, Hanxu et al. [21] considered the kinematics and dynamics problems of an omnidirectional spherical robot. Moreover, the authors found the relationship between the maximum angle velocity and the pose of the robot. Cameron and Book [22] studied the kinematics and dynamics model of nonholonomic systems and established a simplified Boltzmann–Hamel equation for both holonomic and nonholonomic systems. The dynamics equations of a spherical mobile robot, called BYQ-III, on an irregular surface were deduced using the Lagrange scheme [23]. Dynamic modelling, stabilization and control of a spherical robot moving on an inclined plane were also considered [24–26]. Azizi and Naderi [27] proposed

a new inner mechanism with three independent actuators for a spherical robot and investigated its modelling and trajectory planning. Optimal motion planning and control of a spherical robot in different environments with/without obstacles employing Bellman's dynamic programming (DP) methodology were recently developed [28–30]. Further, based on reinforcement learning (RL) algorithm and eXtended Classifier Systems (XCS), a model-free methodology was proposed for motion planning of a spherical robot [31,32]. Using fuzzy logic systems, adaptive estimation and nonlinear control of a PDSR were also studied [33,34].

In general, there has been intensive study on design, dynamic modelling and control of robots. A robust adaptive neural tracking control approach was developed for a class of switched affine nonlinear systems using sliding mode and H_∞ methods [35]. Applying the average dwell-time technique, in the presence of model uncertainties and external disturbances, an adaptive integral sliding mode controller was established for switched nonlinear systems [36]. Further, the design, modelling and sliding mode control of multiple cooperative welding robot manipulators (MWRMs), which combine WRMs with the multiple robot manipulators, were studied [37]. Using multi-model switching, a robust adaptive control scheme was built for discrete SISO systems with unmodelled dynamics, to improve the robustness and transient response of the system [38]. Based on radial basis function neural network (RBFNN) approximation and Lyapunov stability theory, the robust and adaptive switching control problems of a robotic manipulator with uncertainties and disturbances were also addressed [39–41]. Considering the repetitive task and high precision requirement, the dynamics and trajectory tracking control of cooperative cable parallel manipulators for multiple mobile cranes (CPMMC) were investigated employing a robust iterative learning controller [42].

According to the above review, mathematical modelling and motion control of a PDSR on a variable-slope inclined plane have not been solved and are still controversial. This paper deals with the full dynamic modelling of a PDSR on an inclined plane with a variable slope using the Lagrangian formulation, considering all real conditions, inertias and forces. Due to the nature of the robot, it is a nonholonomic and nonlinear system. Therefore, the terminal sliding mode control (TSMC) algorithm is employed for stabilization control of the robot on the moving inclined plane, while an unknown external disturbance is applied and there are unknown control input limits. The controller design is based on the estimation of a compound disturbance, consisting of the unknown external disturbance and nonsymmetric control input saturation. Simulation results demonstrate that, compared to other methods, the approach is highly promising.

The outline of the paper is as follows. The mathematical model of a PDSR moving on a variable-slope inclined plane is derived in the next section. Section 3 is devoted to motion control of the robot on a moving inclined plane using TSMC. Section 4 provides simulation results.

2 Mathematical model of a PDSR on a variable-slope inclined plane

Using gravity, a PDSR moves based on the centre of mass displacement. A schematic diagram of the mechanism of the robot, comprising a spherical shell, a main shaft, a pendulum and two motors, is represented in Fig. 1a. The main shaft is connected to the shell, while the pendulum is connected to the centre of the main shaft, both by means of bearings. One of the motors, which are attached to the main shaft, is applied to rotate the shaft relative to the shell. The pendulum moves relative to the main shaft by the other motor. When the motors are actuated, the sphere moves using gravitational force since the mass centre of the robot changes. An actual PDSR is indicated in Fig. 1b.

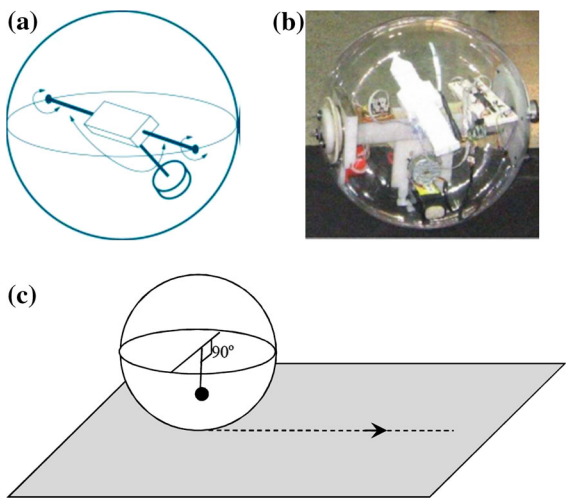

Fig. 1 Mechanism of a PDSR: **a** schematic diagram, **b** a kind of PDSR, **c** moving on a straight line

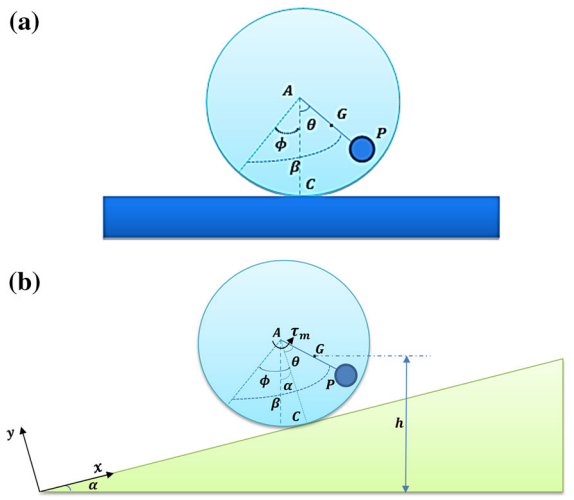

Fig. 2 PDSR side view: **a** on a flat surface, **b** on an inclined plane

Assume that the robot rolls without slipping on a flat surface. For tracing a straight line, the main shaft and the pendulum should be parallel and perpendicular to the surface, respectively. The configuration of the internal mechanism of the robot for this type of motion is shown in Fig. 1c. The second motor for the pendulum is locked and does not move. In other words, the robot moves without any side motion; the angle between the shaft and the pendulum always stays constant, i.e., 90°, as depicted in Fig. 1c. The side view of the robot is illustrated in Fig. 2a. In this figure, points A, C, G and P show, respectively, the centre of the shell, contact point between the robot and the plane, the robot mass centre and the position of the pendulum. Clearly,

$$\beta = \phi + \theta. \tag{1}$$

Now, assuming the spherical robot rolls on a variable-slope inclined plane with the inclination angle $\alpha\,(t)$, as depicted in Fig. 2b, its mathematical model is derived using the Lagrange method.

The Lagrange equation is given as follows:

$$\frac{\mathrm{d}}{\mathrm{d}t}\left(\frac{\partial \mathcal{L}}{\partial \dot{\boldsymbol{q}}}\right) - \frac{\partial \mathcal{L}}{\partial \boldsymbol{q}} = \boldsymbol{Q}, \quad \mathcal{L} = T - V. \tag{2}$$

The total kinetic energy of the system is the sum of kinetic energies of the shell and the pendulum, i.e.,

$$T = T_\mathrm{s} + T_\mathrm{p} \tag{3}$$

$$T_\mathrm{s} = \frac{1}{2} m_\mathrm{s} \|\boldsymbol{V}_\mathrm{A}\|^2 + \frac{1}{2} I_\mathrm{A} \|\boldsymbol{\omega}_\mathrm{s}\|^2 \tag{4}$$

$$T_\mathrm{p} = \frac{1}{2} m_\mathrm{p} \|\boldsymbol{V}_p\|^2, \tag{5}$$

where

$$\boldsymbol{V}_\mathrm{A} = \boldsymbol{V}_\mathrm{C} + \boldsymbol{V}_{A/C}, \quad \boldsymbol{V}_\mathrm{C} = x\dot{\alpha}\boldsymbol{j},$$
$$\boldsymbol{V}_{A/C} = \rho\dot{\phi}\boldsymbol{i}, \quad x = x_0 + \rho\phi \tag{6}$$
$$\boldsymbol{\omega}_\mathrm{s} = \left(\dot{\alpha} - \dot{\phi}\right)\boldsymbol{k} \tag{7}$$
$$\boldsymbol{V}_p = \boldsymbol{V}_\mathrm{A} + \boldsymbol{V}_{p/A},$$
$$\boldsymbol{V}_{p/A} = r\dot{\theta}(\cos(\theta)\,\boldsymbol{i} + \sin(\theta)\boldsymbol{j}). \tag{8}$$

The total potential energy of the system is only associated with the gravity, namely

$$V = Mgh = Mg\,(x\sin(\alpha) + \rho\cos(\alpha) - r_G\cos(\alpha + \theta)) \tag{9}$$

which is positive-definite, since it is measured relative to the horizontal plane and the mass centre of the system is always above this reference ($h > 0$), as shown in Fig. 2b. Note that $x\sin(\alpha) > 0$ and $\rho > r_G$.

To find the generalized forces applied to the system, the method of virtual work is written as

$$\delta W = \tau_m \delta\beta = \tau_m \delta\phi + \tau_m \delta\theta. \tag{10}$$

Hence,

$$Q_\phi = Q_\theta = \tau_m. \tag{11}$$

Substituting the above relations into the Lagrange equation, the model of the system is derived as

$$\left(I_\mathrm{c} + m_\mathrm{p}\rho^2\right)\ddot{\phi} + m_\mathrm{p}\rho r\cos(\theta)\,\ddot{\theta} - I_\mathrm{A}\ddot{\alpha} - m_\mathrm{p}\rho r\sin(\theta)\left(\dot{\theta}^2 + \dot{\theta}\dot{\alpha}\right) - M\rho\,(x_0 + \rho\phi)\,\dot{\alpha}^2 + Mg\rho\sin(\alpha) = \tau_m \tag{12}$$

$$m_\mathrm{p} r^2\ddot{\theta} + m_\mathrm{p}\rho r\cos(\theta)\,\ddot{\phi} + m_\mathrm{p} r\,(x_0 + \rho\phi)\sin(\theta)\,\ddot{\alpha} + m_\mathrm{p}\rho r\sin(\theta)\,\dot{\phi}\dot{\alpha} + Mgr_G\sin(\alpha + \theta) = \tau_m. \tag{13}$$

To find the equilibrium state of the robot, we have

$$r_G\sin(\alpha + \theta) = \rho\sin(\alpha) \tag{14}$$

$$\theta_\mathrm{e} = \sin^{-1}\left(\frac{\rho}{r_G}\sin(\alpha)\right) - \alpha. \tag{15}$$

In other words, when $\theta = \theta_e$, the robot is stable on the inclined plane and does not move. For a variable-slope inclined plane, θ_e is not constant, and hence, θ should track θ_e to stabilize the robot.

3 Motion control of a PDSR on a moving inclined plane applying SMC

This section is divided into two subsections. The TSMC method is briefly described in the next subsection. Subsequently, the algorithm is applied for stabilization control of the robot on the inclined plane.

3.1 The terminal sliding mode control (TSMC) method

Consider the following SISO nonlinear system:

$$\begin{aligned} &\dot{x}_i = x_{i+1}, \quad i = 1, 2, \ldots, n-1 \\ &\dot{x}_n = f(\boldsymbol{x}) + g(\boldsymbol{x})\, u + d \\ &y = x_1, \end{aligned} \tag{16}$$

where $f(\boldsymbol{x})$ and $g(\boldsymbol{x})$ denote two known nonlinear functions. Assume that $g(\boldsymbol{x}) = 0$ for some states, i.e., the control singularity, and the control input has an unknown nonsymmetric saturation, namely

$$u = \begin{cases} u_{\max} & \text{if } v > u_{\max} \\ v & \text{if } u_{\min} \le v \le u_{\max} \\ u_{\min} & \text{if } v < u_{\min}. \end{cases} \tag{17}$$

It can be proved that the robust tracking control input is expressed as [43]

$$v = g(\boldsymbol{x}) \left(g^2(\boldsymbol{x}) + \tau\right)^{-1} v_r, \tag{18}$$

where $\tau > 0$ and v_r will be defined later. Obviously,

$$g^2(\boldsymbol{x}) \left(g^2(\boldsymbol{x}) + \tau\right)^{-1} = 1 - \tau \left(g^2(\boldsymbol{x}) + \tau\right)^{-1}. \tag{19}$$

Substituting v into the system state–space equations, by using the above relation, we have

$$\begin{aligned} \dot{x}_n &= f(\boldsymbol{x}) + g(\boldsymbol{x})(v + \Delta u) + d \\ &= f(\boldsymbol{x}) + v_r + d + g(\boldsymbol{x})\Delta u \\ &\quad - \tau (g^2(\boldsymbol{x}) + \tau)^{-1} v_r, \end{aligned} \tag{20}$$

where $\Delta u = u - v$ is unknown, since it is assumed that the upper and lower limits of the control input are unknown. By defining the compound disturbance as

$$D = d + g(\boldsymbol{x})\Delta u - \tau (g^2(\boldsymbol{x}) + \tau)^{-1} v_r, \tag{21}$$

the following relation is obtained:

$$\dot{x}_n = f(\boldsymbol{x}) + v_r + D. \tag{22}$$

Now, assume that

$$s_1 = y - y_d, \tag{23}$$

where y_d denotes the desired output. The nth time derivative of s_1 is

$$s_1^{(n)} = y^{(n)} - y_d^{(n)} = \dot{x}_n - y_d^{(n)}. \tag{24}$$

Considering this relation, the recursive method of the TSMC of uncertain nonlinear systems is written as [44]

$$\begin{aligned} &s_2 = \dot{s}_1 + \alpha_1 s_1 + \beta_1 s_1^{\frac{p_1}{q_1}} \\ &s_3 = \dot{s}_2 + \alpha_2 s_2 + \beta_2 s_2^{\frac{p_2}{q_2}} \\ &\ldots \\ &s_n = \dot{s}_{n-1} + \alpha_{n-1} s_{n-1} + \beta_{n-1} s_{n-1}^{\frac{p_{n-1}}{q_{n-1}}} + s, \end{aligned} \tag{25}$$

where $\alpha_i > 0$ and $\beta_i > 0$. Also, p_i and q_i are positive odd integers with $p_i < q_i$. The first time derivative of s_i is

$$\dot{s}_i = \ddot{s}_{i-1} + \frac{\mathrm{d}}{\mathrm{d}t}\left(\alpha_{i-1} s_{i-1} + \beta_{i-1} s_{i-1}^{\frac{p_{i-1}}{q_{i-1}}}\right). \tag{26}$$

Hence, the jth time derivative of s_i is

$$s_i^{(j)} = s_{i-1}^{(j+1)} + \frac{d^{(j)}}{dt^{(j)}}\left(\alpha_{i-1} s_{i-1} + \beta_{i-1} s_{i-1}^{\frac{p_{i-1}}{q_{i-1}}}\right). \tag{27}$$

The first time derivative of s_n is given by

$$\begin{aligned} \dot{s}_n &= s_1^{(n)} + \sum_{j=1}^{n-1} \alpha_j s_j^{(n-j)} \\ &\quad + \sum_{j=1}^{n-1} \beta_j \frac{d^{(n-j)}}{dt^{(n-j)}}\left(s_j^{\frac{p_j}{q_j}}\right) + \dot{s}. \end{aligned} \tag{28}$$

Thus,

$$\begin{aligned}\dot{s}_n &= \dot{x}_n - y_d^{(n)} + \sum_{j=1}^{n-1} \alpha_j s_j^{(n-j)} \\ &\quad + \sum_{j=1}^{n-1} \beta_j \frac{d^{(n-j)}}{dt^{(n-j)}} \left(s_j^{\frac{p_j}{q_j}} \right) + \dot{s} \\ &= f(\boldsymbol{x}) + v_r + D - y_d^{(n)} \\ &\quad + \sum_{j=1}^{n-1} \alpha_j s_j^{(n-j)} + \sum_{j=1}^{n-1} \beta_j \frac{d^{(n-j)}}{dt^{(n-j)}} \left(s_j^{\frac{p_j}{q_j}} \right) + \dot{s}.\end{aligned} \tag{29}$$

To estimate the unknown compound disturbance, consider

$$s = z - x_n, \tag{30}$$

where z is obtained from

$$\dot{z} = -ks - \gamma \operatorname{sign}(s) - \epsilon s^{\frac{p_0}{q_0}} - |f(\boldsymbol{x})| \operatorname{sign}(s) + v_r \tag{31}$$

where p_0 and q_0 are positive odd integers with $p_0 < q_0$. As well, k, γ and ϵ are positive and $\gamma \geq |D|$.

It can be proved that the terminal sliding mode disturbance estimate of D is [43]

$$\begin{aligned}\widehat{D} &= -ks - \gamma \operatorname{sign}(s) - \epsilon s^{\frac{p_0}{q_0}} \\ &\quad - |f(\boldsymbol{x})| \operatorname{sign}(s) - f(\boldsymbol{x}).\end{aligned} \tag{32}$$

Applying the output of the disturbance estimator, the terminal sliding mode tracking control is designed as

$$\begin{aligned}v_r &= -f(\boldsymbol{x}) + y_d^{(n)} - \sum_{j=1}^{n-1} \alpha_j s_j^{(n-j)} \\ &\quad - \sum_{j=1}^{n-1} \beta_j \frac{d^{(n-j)}}{dt^{(n-j)}} \left(s_j^{\frac{p_j}{q_j}} \right) - \widehat{D} - \delta s_n - \mu s_n^{\frac{p_n}{q_n}},\end{aligned} \tag{33}$$

where $\delta > 0$ and $\mu > 0$.

3.2 Motion control of a spherical robot on an inclined plane using TSMC

Assuming the angular velocity and the angular acceleration of the inclined plane are negligible, the mathematical model of the robot reduces to

$$\begin{aligned}&\left(I_c + m_p \rho^2 \right) \ddot{\phi} + m_p \rho r \left(\ddot{\theta} \cos(\theta) - \dot{\theta}^2 \sin(\theta) \right) \\ &\quad + Mg\rho \sin(\alpha) = \tau_m\end{aligned} \tag{34}$$

$$m_p r \left(r\ddot{\theta} + \rho \ddot{\phi} \cos(\theta) \right) + Mgr_G \sin(\alpha + \theta) = \tau_m. \tag{35}$$

Combining these relations, after eliminating $\ddot{\phi}$, we have

$$\begin{aligned}&\left(I_c m_p r^2 + m_p^2 \rho^2 r^2 \sin^2(\theta) \right) \ddot{\theta} \\ &\quad + m_p^2 \rho^2 r^2 \sin(\theta) \cos(\theta) \dot{\theta}^2 \\ &\quad + Mg \left(\left(I_c + m_p \rho^2 \right) r_G \sin(\alpha + \theta) \right. \\ &\quad \left. - m_p \rho^2 r \sin(\alpha) \cos(\theta) \right) \\ &= \left(I_c + m_p \rho^2 - m_p \rho r \cos(\theta) \right) \tau_m.\end{aligned} \tag{36}$$

Assuming $x_1 = \theta$ and $x_2 = \dot{\theta}$, state–space equations can be expressed as

$$\begin{aligned}\dot{x}_1 &= \dot{\theta} = x_2 \\ \dot{x}_2 &= \ddot{\theta} = f(x_1, x_2) + g(x_1, x_2) u + d \\ y &= x_1 = \theta,\end{aligned} \tag{37}$$

where

$$\begin{aligned}f(x_1, x_2) &= -\frac{m_p^2 \rho^2 r^2 \sin(x_1) \cos(x_1) x_2^2}{I_c m_p r^2 + m_p^2 \rho^2 r^2 \sin^2(x_1)} \\ &\quad + \frac{Mgr_G \left(I_c + m_p \rho^2 \right) \sin(\alpha + x_1)}{I_c m_p r^2 + m_p^2 \rho^2 r^2 \sin^2(x_1)} \\ &\quad - \frac{Mm_p g \rho^2 r \sin(\alpha) \cos(x_1)}{I_c m_p r^2 + m_p^2 \rho^2 r^2 \sin^2(x_1)} \\ g(x_1, x_2) &= \frac{I_c + m_p \rho^2 - m_p \rho r \cos(x_1)}{I_c m_p r^2 + m_p^2 \rho^2 r^2 \sin^2(x_1)},\end{aligned}$$

with $u = \tau_m$ and d denoting an unknown external disturbance. Assuming u is saturated by unknown limits, the TSMC algorithm is summarized as follows:

$$\begin{aligned}s &= z - x_2 = z - \dot{\theta} \\ \dot{z} &= -ks - \gamma \operatorname{sign}(s) - \epsilon s^{\frac{p_0}{q_0}} \\ &\quad - |f(x_1, x_2)| \operatorname{sign}(s) + v_r \\ s_1 &= y - y_d = x_1 - y_d = \theta - y_d \\ s_2 &= \dot{s}_1 + \alpha_1 s_1 + \beta_1 s_1^{\frac{p_1}{q_1}} + s \\ \widehat{D} &= -ks - \gamma \operatorname{sign}(s) - \epsilon s^{\frac{p_0}{q_0}} \\ &\quad - |f(x_1, x_1)| \operatorname{sign}(s) - f(x_1, x_2)\end{aligned}$$

$$v_r = -f(x_1, x_2) + \ddot{y}_d - \alpha_1 \dot{s}_1 - \beta_1 \frac{\mathrm{d}}{\mathrm{d}t}\left(s_1^{\frac{p_1}{q_1}}\right) - \widehat{D} - \delta s_2 - \mu s_2^{\frac{p_2}{q_2}}$$

$$v = g(x_1, x_2)\left(g^2(x_1, x_2) + \tau\right)^{-1} v_r.$$

The next section provides simulation results of applying the designed controller.

4 Simulation results

This section is devoted to simulation results to demonstrate the effectiveness of the TSMC approach for motion control of a PDSR on a variable-slope inclined plane with an unknown external disturbance and the unknown nonsymmetric input saturation.

Assume that the time-varying external disturbance applied to the system is $d(t) = 3 + 2\sqrt{2}\sin\left(\frac{\sqrt{3}t}{2} + \frac{\pi}{6}\right)$, while the lower and upper limits of the control input are $u_{\min} = -1\,\mathrm{N\,m}$ and $u_{\max} = 1.5\,\mathrm{N\,m}$, and the design parameters to be $k = 1000$, $\gamma = 10$, $\epsilon = 0.8$, $p_0 = 7$, $q_0 = 9$, $\alpha_1 = 100$, $\beta_1 = 0.7$, $p_1 = 3$, $q_1 = 5$, $p_2 = 3$, $q_2 = 5$, $\delta = 100$ and $\mu = 0.6$. The results of applying the TSMC technique for stabilizing the robot on the inclined plane when the slope is constant, i.e., $\alpha = \frac{\pi}{8}$, are represented in Figs. 3, 4 and 5. As mentioned previously, the equilibrium state of the robot is when $\theta = \theta_e = \sin^{-1}(\rho / r_G \sin(\alpha(t))) - \alpha(t)$, which is the desired output y_d, i.e., $y_d = \theta_e$. The comparison result between the output of the system and the desired output are shown in Fig. 3, while the tracking error is indicated in Fig. 4. As depicted in Fig. 5, the control input is bounded between $u_{\min}$ and $u_{\max}$.

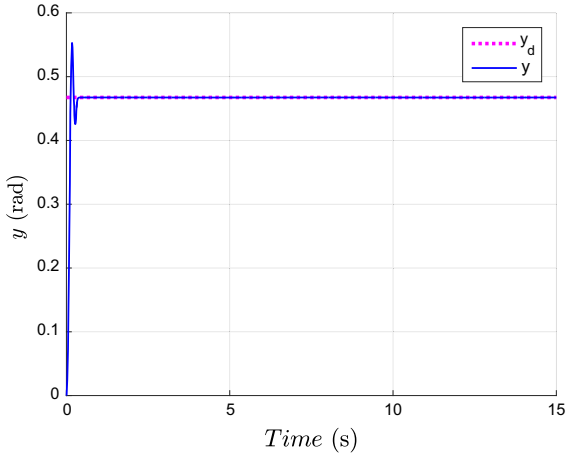

Fig. 3 Output for a constant inclination angle (with input saturation)

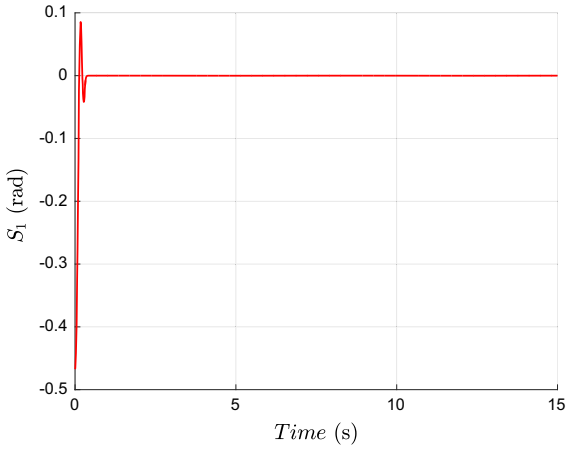

Fig. 4 Tracking error a constant inclination angle (with input saturation)

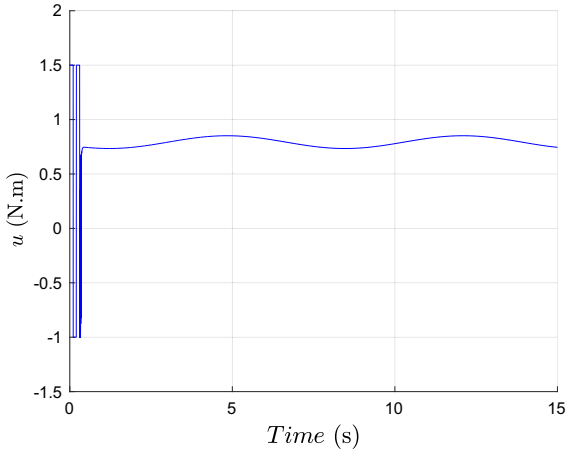

Fig. 5 Control input for a constant inclination angle (with input saturation)

According to Figs. 3, 4 and 5, the tracking error converges to zero in a short time (less than one second), which demonstrates the performance of the disturbance observer-based TSMC. In fact, the method is very promising for uncertain SISO nonlinear systems with a time-varying unknown external disturbance, while there are unknown control input saturation bounds.

Now, assuming the slope of the inclined plane is changing continuously by $\alpha(t) = \frac{\pi}{8} + \frac{\pi}{12}\sin\left(\frac{\pi t}{40}\right)$, namely y_d is not constant, the simulation results are represented in Figs. 6, 7 and 8. Although there is a

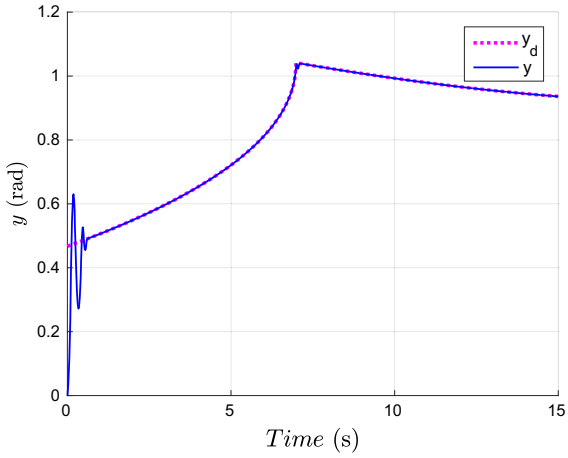

Fig. 6 Output for a variable inclination angle (with input saturation)

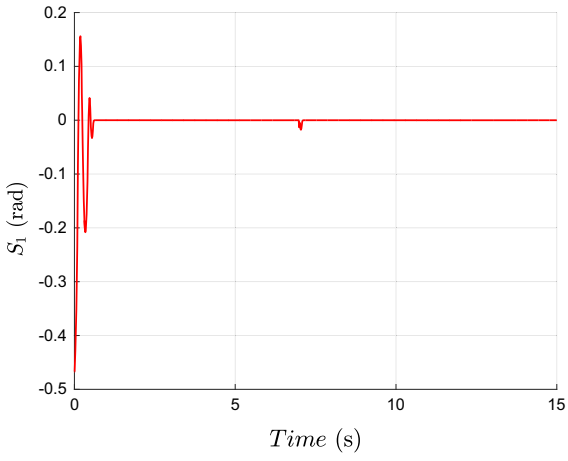

Fig. 7 Tracking error for a variable inclination angle (with input saturation)

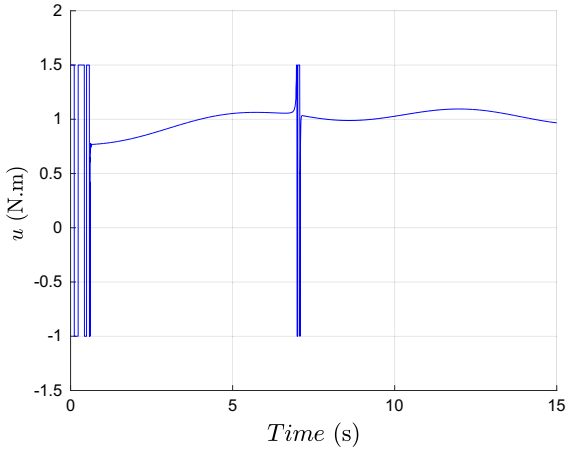

Fig. 8 Control input for a variable inclination angle (with input saturation)

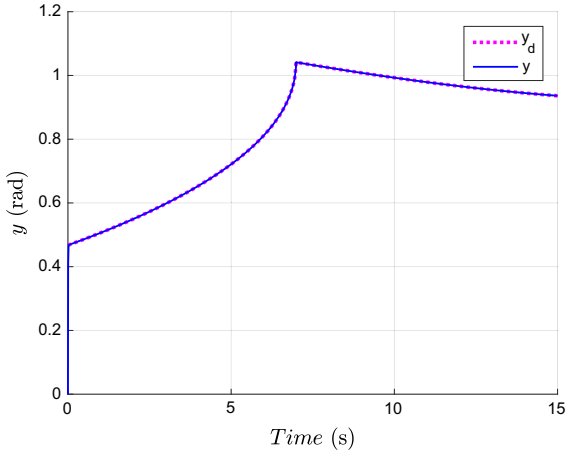

Fig. 9 Output for a variable inclination angle (without input saturation)

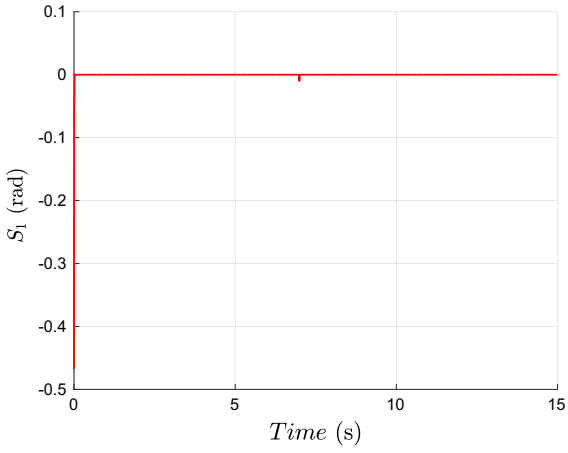

Fig. 10 Tracking error for a variable inclination angle (without input saturation)

jump in the slope of y_d, the tracking error vanishes in a short time.

If there is no saturation on the control input, the tracking error will go to zero much sooner, as illustrated in Figs. 9 and 10. However, the control input increases substantially, which is not practical and cannot be implemented in the real world. In fact, the main advantage of TSMC is tracking control while there are control input limits, which is a significant concern in experimental work. Furthermore, the TSMC demonstrates the Lyapunov stability of the closed-loop system in the presence of input saturation.

Another widely used scheme to control nonlinear systems is sliding mode control (SMC) [45,46].

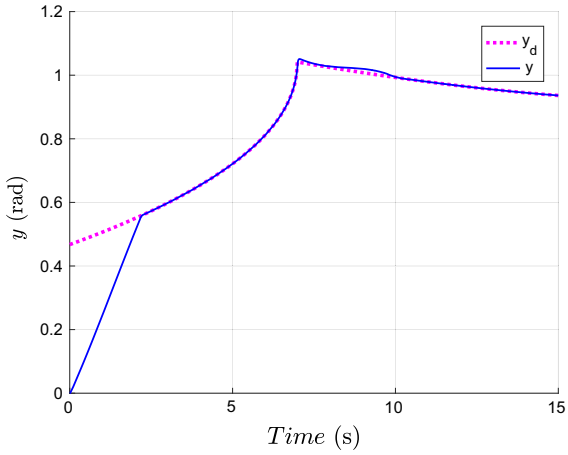

Fig. 11 Output for a variable inclination angle using SMC (with input saturation)

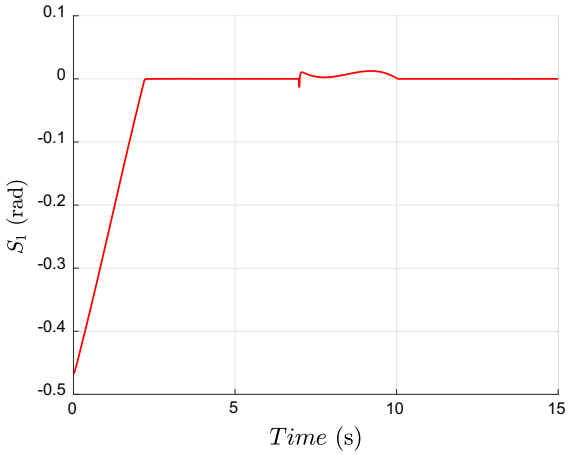

Fig. 12 Tracking error for a variable inclination angle using SMC (with input saturation)

The simulation results of applying SMC to control the motion of a PDSR on a variable-slope inclined plane, with the same unknown external disturbance and input saturation limits, are illustrated in Figs. 11, 12 and 13. As observed in these figures, compared to the results obtained with the TSMC, the tracking error of the SMC is higher; namely, it converges gradually, since the disturbance and the control input limits, which are inevitable in practical implementation, are not estimated. As well, the chattering of the control input of the SMC is much more than that of TMSC, which makes implementation in the real world infeasible due to the limitations of the actuators.

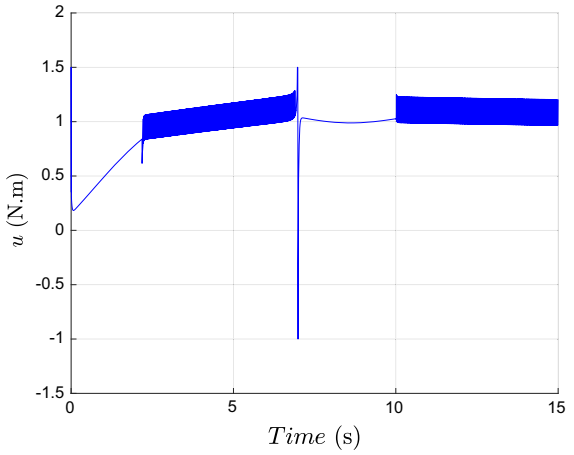

Fig. 13 Control input for a variable inclination angle using SMC (with input saturation)

5 Conclusions

Mathematical modelling and motion control of a PDSR on an inclined plane with a variable slope was developed. The dynamics model was derived applying the Lagrange approach. A compound disturbance, including the unknown external disturbance and the unknown nonsymmetric input saturation, was defined and then estimated using the terminal sliding mode disturbance observer. Next, based on the output of the estimator, the terminal sliding mode control (TSMC) scheme was employed for stabilization control of the robot on the moving inclined plane. Simulation results of applying the TSMC algorithm for tracking control of this uncertain nonlinear system were very promising; the tracking error converged to zero in less than one second, while there were an unknown external disturbance and nonsymmetric control input limits, which guarantee the feasibility of implementing the technique in the real world. Future research may include actual implementation of the TSMC approach on the prototype PDSR moving on a variable-slope inclined plane.

References

1. Armour, R.H., Vincent, J.F.: Rolling in nature and robotics: a review. J. Bionic Eng. **3**(4), 195–208 (2006)
2. Zhan, Q., Zhou, T., Chen, M., Cai, S.: Dynamic trajectory planning of a spherical mobile robot. In: 2006 IEEE Conference on Robotics, Automation and Mechatronics, pp. 1–6. IEEE (2006)

3. Zhan, Q., Cai, Y., Liu, Z.: Near-optimal trajectory planning of a spherical mobile robot for environment exploration. In: 2008 IEEE Conference on Robotics, Automation and Mechatronics, pp. 84–89. IEEE (2008)
4. Cai, Y., Zhan, Q., Xi, X.: Path tracking control of a spherical mobile robot. Mech. Mach. Theory **51**, 58–73 (2012)
5. Mahboubi, S., Fakhrabadi, M.M.S., Ghanbari, A.: Design and implementation of a novel spherical mobile robot. J. Intell. Robot. Syst. **71**(1), 43–64 (2013)
6. Peng, Z., Wen, G., Yang, S., Rahmani, A.: Distributed consensus-based formation control for nonholonomic wheeled mobile robots using adaptive neural network. Nonlinear Dyn. **86**(1), 605–622 (2016)
7. Tayefi, M., Geng, Z., Peng, X.: Coordinated tracking for multiple nonholonomic vehicles on SE (2). Nonlinear Dyn. **87**(1), 665–675 (2017)
8. Li, Z., Canny, J.: Motion of two rigid bodies with rolling constraint. IEEE Trans. Robot. Autom. **6**(1), 62–72 (1990)
9. Mojabi, P.: Introducing August: a novel strategy for an omnidirectional spherical rolling robot. In: IEEE International Conference on Robotics and Automation, 2002. Proceedings. ICRA'02, vol. 4, pp. 3527–3533. IEEE (2002)
10. Bhattacharya, S., Agrawal, S.K.: Design, experiments and motion planning of a spherical rolling robot. In: IEEE International Conference on Robotics and Automation, 2000. Proceedings. ICRA'00, vol. 2, pp. 1207–1212. IEEE (2000)
11. Bhattacharya, S., Agrawal, S.K.: Spherical rolling robot: a design and motion planning studies. IEEE Trans. Robot. Autom. **16**(6), 835–839 (2000)
12. Halme, A., Schonberg, T., Wang, Y.: Motion control of a spherical mobile robot. In: 1996 4th International Workshop on Advanced Motion Control, 1996. AMC'96-MIE. Proceedings, vol. 1, pp. 259–264. IEEE (1996)
13. Halme, A., Suomela, J., Schönberg, T., Wang, Y.: A spherical mobile micro-robot for scientific applications. In: ASTRA, 96 (1996)
14. Bicchi, A., Balluchi, A., Prattichizzo, D., Gorelli, A.: Introducing the "SPHERICLE": an experimental testbed for research and teaching in nonholonomy. In: 1997 IEEE International Conference on Robotics and Automation, 1997. Proceedings, vol. 3, pp. 2620–2625. IEEE (1997)
15. Marigo, A., Bicchi, A.: A local-local planning algorithm for rolling objects. In: Robotics and Automation, 2002. IEEE International Conference on Proceedings. ICRA'02, vol. 2, pp. 1759–1764. IEEE (2002)
16. Joshi, V.A., Banavar, R.N.: Motion analysis of a spherical mobile robot. Robotica **27**(03), 343–353 (2009)
17. Joshi, V.A., Banavar, R.N., Hippalgaonkar, R.: Design and analysis of a spherical mobile robot. Mech. Mach. Theory **45**(2), 130–136 (2010)
18. Liu, D., Sun, H., Jia, Q.: A family of spherical mobile robot: driving ahead motion control by feedback linearization. In: 2nd International Symposium on Systems and Control in Aerospace and Astronautics, 2008. ISSCAA 2008, pp. 1–6. IEEE (2008)
19. Qiang, Z., Chuan, J., Xiaohui, M., Yutao, Z.: Mechanism design and motion analysis of a spherical mobile robot. Chin. J. Mech. Eng. **18**(4), 542–545 (2005)
20. Qiang, Z., Zengbo, L., Yao, C.: A back-stepping based trajectory tracking controller for a non-chained nonholonomic spherical robot. Chin. J. Aeronaut. **21**(5), 472–480 (2008)
21. Hanxu, S., Aiping, X., Qingxuan, J., Liangqing, W.: Omnidirectional kinematics analysis on bi-driver spherical robot. J. Beijing Univ. Aeronaut. Astronaut. **31**(7), 735 (2005)
22. Cameron, J.M., Book, W.J.: Modeling mechanisms with nonholonomic joints using the Boltzmann-Hamel equations. Int. J. Robot. Res. **16**(1), 47–59 (1997)
23. Yu, T., Sun, H., Zhang, Y.: Dynamic analysis of a spherical mobile robot in rough terrains. In: SPIE Defense, Security, and Sensing (pp. 80440V-80440V). International Society for Optics and Photonics (2011)
24. Yu, T., Sun, H., Zhang, Y., Zhao, W.: Control and stabilization of a pendulum-driven spherical mobile robot on an inclined plane. In: Proceedings of 11th International Symposium on Artificial Intelligence, Robotics and Automation in Space (2012)
25. Yu, T., Sun, H., Jia, Q., Zhang, Y., Zhao, W.: Stabilization and control of a spherical robot on an inclined plane. Res. J. Appl. Sci. Eng. Technol. **5**(6), 2289–2296 (2013)
26. Roozegar, M., Mahjoob, M.J.: Modelling and control of a non-holonomic pendulum-driven spherical robot moving on an inclined plane: simulation and experimental results. IET Control Theory Appl. **11**, 541–549 (2017)
27. Azizi, M.R., Naderi, D.: Dynamic modeling and trajectory planning for a mobile spherical robot with a 3Dof inner mechanism. Mech. Mach. Theory **64**, 251–261 (2013)
28. Roozegar, M., Mahjoob, M.J., Shafiekhani, A.: using dynamic programming for path planning of a spherical mobile robot. In: International Conference on Advances in Control Engineering, Istanbul, Turkey (2013)
29. Roozegar, M., Mahjoob, M.J., Jahromi, M.: DP-based path planning of a spherical mobile robot in an environment with obstacles. J. Frankl. Inst. **351**(10), 4923–4938 (2014)
30. Roozegar, M., Mahjoob, M.J., Jahromi, M.: Optimal motion planning and control of a nonholonomic spherical robot using dynamic programming approach: simulation and experimental results. Mechatronics **39**, 174–184 (2016)
31. Esfandyari, M.J., Roozegar, M., Panahi, M.S., Mahjoob, M.: Motion planning of a spherical robot using eXtended Classifier Systems. In: 2013 21st Iranian Conference on Electrical Engineering (ICEE), pp. 1–6. IEEE (2013)
32. Roozegar, M., Mahjoob, M.J., Esfandyari, M.J., Panahi, M.S.: XCS-based reinforcement learning algorithm for motion planning of a spherical mobile robot. Appl. Intell. **45**(3), 736–746 (2016)
33. Taheri-Andani, M., Mahjoob, M.J., Ayati, M.: Control of a spherical mobile robot using sliding mode and fuzzy sliding mode controllers. In: 2016 1st International Conference on New Research Achievements in Electrical and Computer Engineering, Tehran, Iran. IEEE (2016)
34. Roozegar, M., Mahjoob, M.J., Ayati, M.: Adaptive estimation of nonlinear parameters of a nonholonomic spherical robot using a modified fuzzy-based speed gradient algorithm. Regul. Chaotic Dyn. **22**(3), 226–238 (2017)
35. Yu, L., Fei, S., Li, X.: Robust adaptive neural tracking control for a class of switched affine nonlinear systems. Neurocomputing **73**(10), 2274–2279 (2010)
36. Yu, L., Zhang, M., Fei, S.: Non-linear adaptive sliding mode switching control with average dwell-time. Int. J. Syst. Sci. **44**(3), 471–478 (2013)

37. Zi, B., Sun, H., Zhu, Z., Qian, S.: The dynamics and sliding mode control of multiple cooperative welding robot manipulators. Int. J. Adv. Robot. Syst. **9**(53), 1–10 (2012)
38. Yu, L., Fei, S., Qian, W.: Robust adaptive control for single input/single output discrete systems via multi-model switching. Proc. Inst. Mech. Eng. Part I J. Syst. Control Eng. **228**(1), 42–48 (2014)
39. Yu, L., Fei, S.: Robustly stable switching neural control of robotic manipulators using average dwell-time approach. Trans. Inst. Meas. Control **36**(6), 789–796 (2014)
40. Yu, L., Fei, S., Sun, L., Huang, J.: An adaptive neural network switching control approach of robotic manipulators for trajectory tracking. Int. J. Comput. Math. **91**(5), 983–995 (2014)
41. Yu, L., Fei, S., Sun, L., Huang, J., Yang, G.: Design of robust adaptive neural switching controller for robotic manipulators with uncertainty and disturbances. J. Intell. Robot. Syst. **77**(3–4), 571–581(2015)
42. Qian, S., Zi, B., Ding, H.: Dynamics and trajectory tracking control of cooperative multiple mobile cranes. Nonlinear Dyn. **83**(1–2), 89–108 (2016)
43. Chen, M., Wu, Q.X., Cui, R.X.: Terminal sliding mode tracking control for a class of SISO uncertain nonlinear systems. ISA Trans. **52**(2), 198–206 (2013)
44. Yu, X., Zhihong, M.: Fast terminal sliding-mode control design for nonlinear dynamical systems. IEEE Trans. Circuits Syst. I Fundam. Theory Appl. **49**(2), 261–264 (2002)
45. Aliakbari, S., Ayati, M., Osman, J.H., Sam, Y.M.: Second-order sliding mode fault-tolerant control of heat recovery steam generator boiler in combined cycle power plants. Appl. Therm. Eng. **50**(1), 1326–1338 (2013)
46. Liu, J., Wang, X.: Advanced Sliding Mode Control for Mechanical Systems: Design, Analysis and MATLAB Simulation. Springer Science & Business Media, Berlin (2012)